

Polynomial Regression Calibration Method of Total Dissolved Solids Sensor for Hydroponic Systems

Ansar Jamil*, Teo Sheng Ting, Zuhairiah Zainal Abidin, Maisara Othman, Mohd Helmy Abdul Wahab, Mohammad Faiz Liew Abdullah, Mariyam Jamilah Homam, Lukman Hanif Muhammad Audah and Shaharil Mohd Shah

Advanced Telecommunication Research Center (ATRC), Universiti Tun Hussein Onn Malaysia, Johor, Malaysia

ABSTRACT

Smart hydroponic systems have been introduced to allow farmers to monitor their hydroponic system conditions anywhere and anytime using Internet of Things (IoT) technology. Several sensors are installed on the system, such as Total Dissolved Solids (TDS), nutrient level, and temperature sensors. These sensors must be calibrated to ensure correct and accurate readings. Currently, calibration of a TDS sensor is only possible at one or a very small range of TDS values due to the very limited measurement range of the sensor. Because of this, we propose a TDS sensor calibration method called Sectioned-Polynomial Regression (Sec-PR). The main aim is to extend the measurement range of the TDS sensor and still provide a good accuracy of the sensor reading. Sec-PR computes the polynomial regression line that fits into the TDS sensor values. Then, it divides the regression line into several sections. Sec-PR calculates the average ratio between the polynomial regressed TDS sensor values and the TDS meter in each section. These average ratio values map the TDS sensor reading to the TDS meter. The performance of Sec-PR was determined using mathematical analysis and verified using

experiments. The finding shows that Sec-PR provides a good calibration accuracy of about 91% when compared to the uncalibrated TDS sensor reading of just 78% with Mean Average Error (MAE) and Root Mean Square Error (RMSE) equal to 59.36 and 93.69 respectively. Sec-PR provides a comparable performance with Machine Learning and Multilayer Perception method.

Keywords: Calibration, hydroponic, polynomial regression, TDS sensor

ARTICLE INFO

Article history:

Received: 09 October 2022

Accepted: 04 April 2023

Published: 08 September 2023

DOI: <https://doi.org/10.47836/pjst.31.6.08>

E-mail addresses:

ansar@uthm.edu.my (Ansar Jamil)

shengting97@gmail.com (Teo Sheng Ting)

zuhairia@uthm.edu.my (Zuhairiah Zainal Abidin)

maisara@uthm.edu.my (Maisara Othman)

helmy@uthm.edu.my (Mohd Helmy Abdul Wahab)

faiz@uthm.edu.my (Mohammad Faiz Liew Abdullah)

mariyam@uthm.edu.my (Mariyam Jamilah Homam)

hanif@uthm.edu.my (Lukman Hanif Muhammad Audah)

shaharil@uthm.edu.my (Shaharil Mohd Shah)

* Corresponding author

INTRODUCTION

Agriculture is one of the most productive sectors in Malaysia, especially palm oil. As of 2021, Malaysia is the world's second-largest palm oil producer and exporter after Indonesia. It is about 26% of world production and 34% of world export in 2020 (<https://www.trade.gov/malaysia-country-commercial-guide>). As additional land for palm oil production is unavailable, the same goes for other types of agriculture, such as vegetables, paddy, rice, and fruits. Any large-scale deforestation for agriculture is prohibited due to the negative impact on nature. However, food security issues after covid-19 experienced by many countries caused shortages in the supply of food items such as chicken, vegetables, and cooking oil. As a result, the increase in food prices burdens Malaysians, and because of that, agriculture is one of the pillars of Malaysia's economy.

A hydroponic system is a suitable solution to tackle this critical issue. Hydroponic is a subset of horticulture that uses mineral nutrient solution as a medium for the cultivation of crops instead of soil (Domingues et al., 2012; Maucieri et al., 2019). Any medium other than soil, such as sand, gravel, pebbles, perlite, rock wool, or aquatic medium, could also hold the plant (Garg et al., 2021). Hydroponics requires small space areas without the need for a large land clearing. Hydroponics can be installed in a small yard and a building with proper lighting for indoor farming. There are different types of hydroponic systems, which are the Nutrient Film Technique (NFT) (Alipio et al., 2019; Graves, 1983), Ebb and Flow system (Daud et al., 2018); Wick System (Dubey & Nain, 2020), Deep Flow Technique (DFT) (Pramono et al., 2020) and drip hydroponic (Olubanjo et al., 2022). It is very important to manage water and nutrients in the hydroponic system to achieve the optimum growth of crops (Son et al., 2020). The concentration of ions in the nutrient solutions reduces with time as it is absorbed by plants, which is measured according to electrical conductivity (EC) characteristics (Hosseini et al., 2021; Singh & Dunn, 2016). A high concentration of ions provides good electrical conductivity. Otherwise, a low concentration of ions provides poor electrical conductivity. Instead of EC, other parameters such as pH, dissolved oxygen, and temperature should be measured. Analysis of nutrient solutions and adjustment of nutrient ratios must be done every day for a correct nutrient reading. With the advancement of technologies, IoT technology could be implemented to ease collecting these nutrient parameters automatically, which can be viewed using a web server or phone app. IoT technology transforms conventional hydroponic into smart hydroponic systems (Modu et al., 2020; Munandar et al., 2018).

A smart hydroponic system can be realized and applied at all levels, whether on a small scale at home or a large scale commercially. Farmers can be anywhere away from the hydroponic farm but still be able to monitor the condition of their farm, and if needed, they can manually control it themselves. An IoT device is installed in an existing hydroponic system. Sensors are attached to the IoT devices, such as TDS/EC sensors, pH sensors,

oxygen sensors, and liquid level sensors, to measure the parameter of the hydroponic system. It is critical to ensure that these connected sensors are calibrated during the installation and while the system operates. Failure to ensure that each sensor is regularly and accurately calibrated will result in inaccurate sensor readings. If this situation occurs, the IoT device does not work properly, causing a failure to the entire smart hydroponic system that will cause decreases in crop yield.

Let us consider a TDS sensor, the easiest method to calibrate this sensor is using a reference TDS meter. Reference TDS meter means that this instrument has been calibrated using standard solutions (alkaline, neutral, and acidic solutions), which are normally included at the time of purchase. Several brands of TDS meters are available in the market, such as Hanna TDS instrument tester and Xiaomi portable TDS meter. Manual calibration of a TDS sensor is a simple process. First, use a TDS meter to prepare a nutrient solution at the required TDS value measures in ppm (part per million) units. Second, deep the uncalibrated TDS sensor into the solution and take the sensor reading. Third, calculate the offset by deducting the sensor reading from the TDS meter reading, and finally, add the offset to the sensor reading to make the sensor reading almost the same as the TDS meter reading. For example, if the required level is 1000 ppm, a nutrient solution is prepared at this level using the TDS meter. It means the TDS meter reading is also 1000 ppm. When the TDS sensor is deep into the nutrient solution, the sensor reading is 900 ppm. Here, the offset is 100 ppm should be added to the sensor reading to achieve the required level. However, this method is only valid at one TDS value. The calibration process must be repeated if the required TDS value is changed.

Suseno et al. (2020) developed a calibration method for TDS sensors for nutrient concentrations up to 780 ppm. They characterized analog TDS sensor readings and standard TDS values. After that, the calibration is performed by comparing the data read by the analog TDS sensor with data from the standard TDS results. The characterization graph shows the linear equation between the x-axis variable, namely the ADC reading, and the y-axis, the standard multimeter voltage value. The relationship between the ADC reading with the standard voltage value produces an equation.

Wibowo et al. (2019) proposed a nutrient dosing system for aquaponic that is very important to improve the quality of catfish and lettuce yield. The dosing system must ensure that the nutrient level is between 400 ppm and 500 ppm. The TDS sensor was calibrated so the TDS sensor reading is the same as the TDS meter. Then, the calibration accuracy is calculated by observing the systematic errors. The calibration range of the TDS sensor is up to 819 ppm.

Nguyen et al. (2018) shared a case study about calibrating conductivity sensors using Combined Algorithm Selection and Hyperparameter Optimization. A different model of calibration process was carried out by using the Gaussian process (Franchini et al., 2019;

Peršić et al., 2021; Urban et al., 2015), Simple Logistic (Zheng et al., 2019) and Linear Regression (Iida et al., 2020; Koestoer et al., 2019). Based on their finding, the calibration range of the TDS sensor is within 200 ppm to 2000 ppm only. At the same time, the uncalibrated TDS sensor has a minimum of 57 and a maximum of 1756.92.

In this paper, we propose a new TDS calibration method called Sectioned-Polynomial Regression (Sec-PR) to extend the measurement range of the TDS sensor over the specification by the manufacturer. We just considered the calibration range from 0 to 3000 ppm in this research work. However, the Sec-PR calibration range can be extended to more than 3000 ppm, depending on applications. It is expected that Sec-PR will be able to provide a good calibration accuracy when compared to the existing methods, such as linear regression, multi-layer perception, and the Gaussian process. In addition, Sec-PR is expected to be implemented easily into the programming code of smart hydroponic systems.

METHODOLOGY

The methodology in this work can be divided into three phases: the initial experiment, mathematical analysis, and implementation of Sec-PR. For the initial experiment phase, an experiment was conducted to compare the TDS sensor and TDS meter readings over different concentrations of fertilizer. This step is very important to determine the trend of the TDS sensor and TDS meter reading used in the next phase. In this mathematical analysis phase, the Sec-PR calibration method is designed to make the TDS sensor reading the same as the TDS meter reading over a wide measurement range. Microsoft Excel was used during the design to analyze the calibration accuracy of Sec-PR. Modifications to the Sec-PR design can be optimized to achieve its best performance. The next phase is the process where Sec-PR is applied to the program code, and the performance of Sec-PR is determined in the actual experiment, which is the same experiment as in the first phase. The TDS sensor reading from the Sec-PR is compared with the TDS meter reading, and the accuracy of the reading is determined. After that, the result is verified with the findings from the second phase, which is a mathematical analysis. Furthermore, in this phase, the performance of Sec-PR is compared with the existing calibration methods of the TDS sensor.

Figure 1 shows the experiment configuration to measure a TDS sensor and a TDS meter reading over different concentrations of fertilizer. The experiment configuration consists of a TDS sensor, ESP 32 dev kit, laptop, 25-liter container as the tank, TDS meter, water, and fertilizer AB. The TDS sensor is dipped into the tank, and the other end is connected to the ESP32 dev kit, which is a microcontroller. ESP32 reads the TDS sensor continuously, and the reading is sent to the laptop using serial communication. Then, the reading can be viewed using a serial monitor window. The experiment begins with the container filled with 6 liters of water. Then, the initial reading of the water in the tank, where no fertilizer has

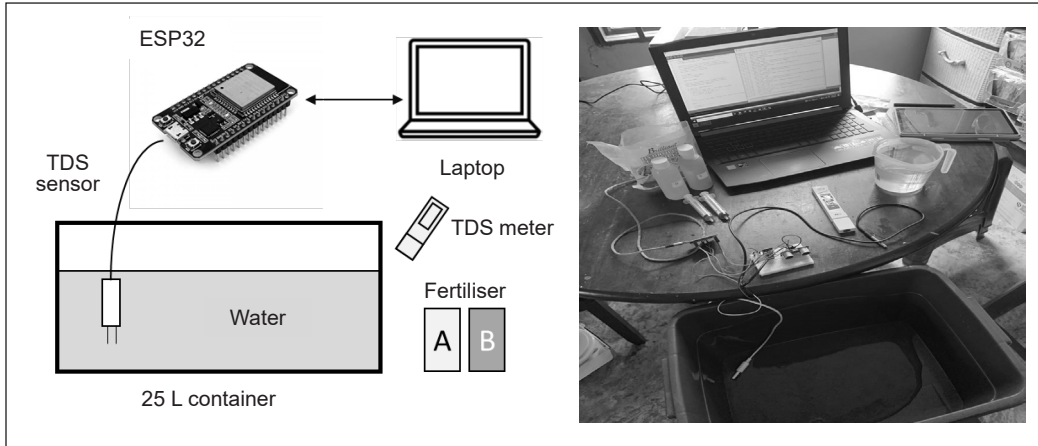


Figure 1. Experiment configuration

been added, is measured using the TDS meter and TDS sensor. After that, add 1 ml of AB fertilizer into the tank using a syringe and stir the solution well. The TDS reading of the nutrient is measured again using the TDS meter and the TDS sensor. This step is repeated by adding another 1 ml of fertilizer AB for fifteen different points until the TDS value is about 3000 ppm. This experiment is repeated five times to increase the accuracy of the data.

TDS value indicates how many milligrams of soluble solids are dissolved in one liter of water. Usually, the higher the TDS value, the higher the number of soluble solids dissolved in water, which means the concentration of the fertilizer is high. Therefore, the TDS value represents one reference point to reflect the fertilizer concentration used widely in hydroponic farms. In this work, we used Gravity Analog TDS Sensors, a consumer-grade product available in the market at an affordable price. The Gravity Analog TDS sensor costs a hundred times cheaper when compared to an industrial-grade TDS sensor. The TDS sensor measures the electrical conductivity of the solution, R , and then ESP32 converts the sensor reading into the TDS value in ppm unit using Equation 1.

$$TDS\ value = (133.42 \times v^3 - 255.86 \times v^2 + 8.57.39 \times v) \times 0.5\ ppm \quad [1]$$

Where v is the compensation voltage calculated based on the sensor reading, R and temperature of the solution, T using Equation 2.

$$v = R / (1.0 + 0.02 (T - 25.0)) \quad [2]$$

Figure 2 shows the TDS sensor reading and TDS meter reading for different concentrations of fertilizer from the initial experimental phase. The TDS sensor provides a nonlinear increase in TDS value. As fertilizer concentration increases, the increment of

TDS value is reduced significantly. As expected, the TDS meter reading increases linearly with the increase in the concentration of fertilizer. Based on the graph, both devices give the same reading at one TDS value of about 2040 ppm. Otherwise, the TDS sensor reading deviates from the TDS meter for other TDS values. For TDS values below 2040 ppm, the TDS sensor reading is higher than the TDS meter reading. For TDS values over 2040 ppm, the sensor reading is lower than the TDS meter reading. The average deviation of the TDS sensor reading from the TDS meter is equal to 243.4 ppm value. Based on the trend of the graph, the deviation of TDS sensor readings from the TDS meter becomes larger for TDS values more than 3000 ppm.

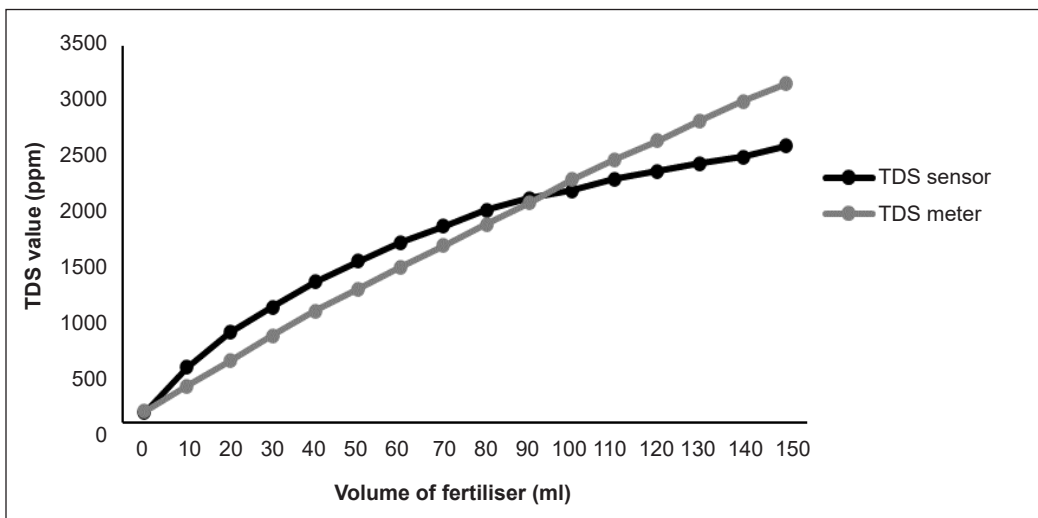


Figure 2. TDS sensor and TDS meter reading over different concentrations of fertilizer

Sectioned-polynomial Regression of TDS Sensor Calibration

A simple way to calibrate the TDS sensor is to offset the TDS sensor reading to make it equal to the TDS meter reading. For example, if the TDS sensor reading is 1440 ppm and the TDS meter reading is 1671 ppm, offset by 231 ppm is added to the TDS sensor reading. Although it is a simple method, this calibration method is suitable for just one calibration point or a very small calibration range of TDS values. For any changes to the calibration setting of TDS values, the TDS sensor must be recalibrated. Another calibration method is to model the TDS sensor readings using linear regression. Linear Regression is the process of finding a line that best fits the data points available on the plot so that we can use it to predict output values for inputs that are not present in the data set we have, with the belief that those outputs would fall on the line (Hope, 2020). While the Least Squares Regression Line is the line that makes the vertical distance from the data points to the regression line as small as possible. It is called a “least square” because the best line of fit is one that

minimizes the variance (the sum of squares of the errors) (Karunasingha, 2022). Figure 3 shows a line graph computed using linear regression for TDS sensor reading. Deviation from the TDS meter is 210 ppm, which is slightly better when compared to the original sensor reading, which is 243 ppm; however, the deviation value still can be considered high due to the non-linearity characteristic of the TDS sensor reading. Because of that, Sec-PR uses the polynomial regression model that fits into the TDS sensor reading with R^2 equal to 0.9946.

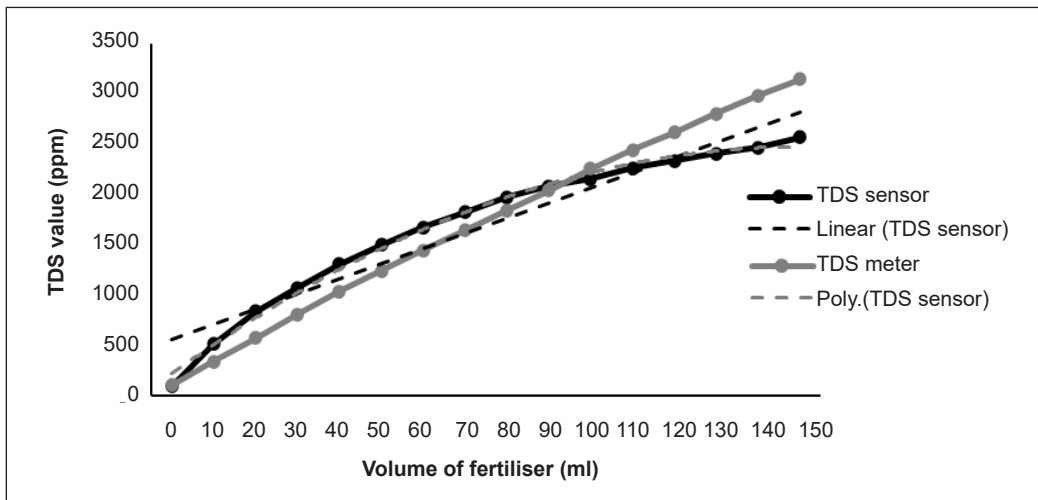


Figure 3. Polynomial regression of TDS sensor reading

Sec-PR maps the TDS sensor reading with the TDS meter reading by dividing the graph into a few sections. The number of sections depends on the TDS sensor reading over different concentrations of fertilizer. The minimum number of sections is two and can exceed several sections required to achieve a wide calibration range with better accuracy. The total TDS sensor readings limit the number of sections. A higher number of sensors reading allows more sections to be created. Otherwise, a smaller number of sensor readings just allows a smaller number of sections. Table 1 shows the Sec-PR calibration algorithm. Each section is labeled as S_i is numbered and represented by where i refers to the number of sections starting from 1 to n . It means that n is the total number of sections. The average ratio between y_i and y_s is calculated for each section and represented by R_i , which determines the calibrated value for the TDS sensor reading, TDS_{cal} . TDS_{cal} is computed by dividing the current TDS sensor reading, TDS_{sensor} , with R_i , where TDS_{sensor} must be within the minimum and maximum TDS value for the i^{th} section, represented as min_i and max_i , respectively. Equation of TDS_{cal} can be implemented easily in the coding by simply using the if-else-if or case function to determine which the current TDS sensor reading belongs to which section.

Let us consider Sec-PR with 3 sections, as shown in Figure 4. The total number of sections, n , equals 3, each labeled S_1 , S_2 , and S_3 . Range of TDS value for S_1 is between and $min_1 = 98.2$ ppm and $max_1 = 1309$ ppm. Range of TDS value for S_2 is between $min_2 = 1310$ and $max_2 = 2081$ ppm. Range of TDS value for S_3 is between $min_3 = 2082$ and $max_3 = 2571$ ppm. Then, Sec-PR calculates the average ratio between the polynomial regression of the TDS sensor with the TDS meter, R_i , for each section. The calculated results for R_1 , R_2 , and R_3 are 1.54, 1.13, and 0.89. TDS_{cal} can be obtained by dividing the current TDS sensor reading with R_i . For example, if the current TDS sensor reading, TDS_{sensor} , is 256 ppm, the reading falls into section S_1 . TDS_{cal} value is calculated by dividing 256 by 1.54, which equals 166 ppm. Another example is if the current TDS sensor reading is 1500 ppm in section S_2 , the TDS_{cal} value becomes 1327 ppm, calculated by dividing 1500 by 1.13.

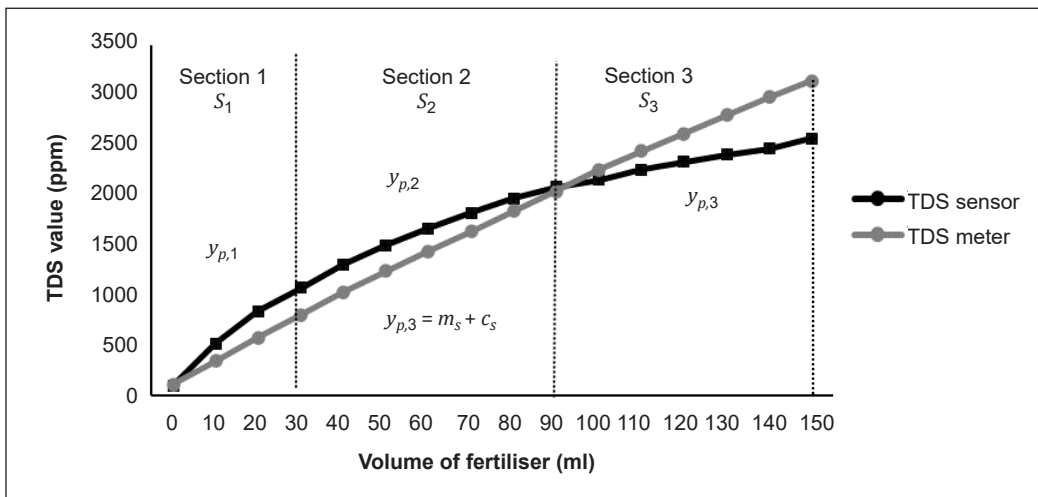


Figure 4. Sec-PR for three sections

Table 1
Sec-PR calibration algorithm

| Sec-PR Algorithm | |
|------------------|--|
| 1 | <p style="text-align: center;">Parameters</p> <p>n is the total number of sections</p> <p>x is the volume of fertilizer</p> <p>S_i i^{th} section</p> <p>TDS_{meter} measured TDS value using the TDS meter</p> <p>TDS_{sensor} measured TDS value using the TDS sensor</p> <p>TDS_{cal} calibrated TDS value from Sec-PR</p> <p>$y_p = \beta_0x + \beta_1x + c$ the second-order polynomial regression line for the TDS sensor</p> <p>$y_{p,i}$ TDS sensor value on the polynomial regression line at i^{th} section</p> <p>min_i is the minimum range of TDS value at i^{th} section</p> <p>max_i is the maximum range of TDS value at i^{th} section</p> |

Table 1 (continue)

| Sec-PR Algorithm | |
|------------------|---|
| 2 | <p style="text-align: center;">Measure standard TDS meter reading</p> $y_s = m_s x + c_s \text{ the linear line for TDS meter reading.}$ |
| 3 | <p style="text-align: center;">Measure TDS sensor reading</p> $y_p = \beta_0 x + \beta_1 x + c \text{ the polynomial regression for TDS sensor reading}$ |
| | Divide TDS sensor reading into n section |
| 4 | <p style="text-align: center;">Polynomial regression at i^{th} section</p> $y_{p,i} = \beta_0 x + \beta_1 x + c$ $i = 1, 2, 3, 4 \dots \dots, n$ |
| 5 | <p style="text-align: center;">Mean ratio between TDS sensor value (on the line of the polynomial regression) and TDS meter for i^{th} section, R_i</p> $R_i = \text{mean} \left(\frac{y_{p,i}(x)}{y_s(x)} \right)$ |
| 6 | <p style="text-align: center;">Calculate the calibration value of the TDS sensor reading for i^{th} section</p> $TDS_{cal} = \frac{TDS_{sensor}}{R_i}, \quad \min_i \leq TDS_{sensor} < \max_i$ <p style="text-align: center;">For n sections, the equation can be written as</p> $TDS_{cal} = \begin{cases} \frac{TDS_{sensor}}{R_1}, & \min_1 \leq TDS_{sensor} < \max_1 \\ \frac{TDS_{sensor}}{R_2}, & \min_2 \leq TDS_{sensor} < \max_2 \\ \frac{TDS_{sensor}}{R_3}, & \min_3 \leq TDS_{sensor} < \max_3 \\ \vdots & \vdots \\ \frac{TDS_{sensor}}{R_n}, & \min_n \leq TDS_{sensor} < \max_n \end{cases}$ |

RESULTS AND DISCUSSION

Figure 5 shows the TDS values of Sec-PR for the different number of sections over the different fertilizer volumes. Sec-PR (6 sections) provides the best performance, with the TDS value being very close to the TDS meter. Sec-PR (6 sections) has recorded MAE and RMSE equal to 51.52 and 62.37, respectively (Table 2). It is about

a 78% improvement compared to the uncalibrated TDS sensor value, with MAE and RMSE equal to 243.34 and 285.41, respectively. Besides that, Sec-PR with a higher number of

Table 2
Mathematical calculation of MAE and RMSE for Sec-PR

| Algorithm | MAE | RMSE |
|----------------------------|--------|--------|
| TDS Sensor | 243.34 | 285.41 |
| Polynomial Regression (PR) | 301.12 | 415.71 |
| Sec-PR (2 Sections) | 141.06 | 182.26 |
| Sec-PR (4 Sections) | 66.60 | 84.99 |
| Sec-PR (6 Sections) | 51.52 | 62.37 |

sections provides better performance when compared to Sec-PR with a lower number of sections. That means Sec-PR (2 sections) provides the lowest performance with MAE and RMSE equal to 141.06 and 182.26, respectively, but still better when compared to the uncalibrated TDS sensor value.

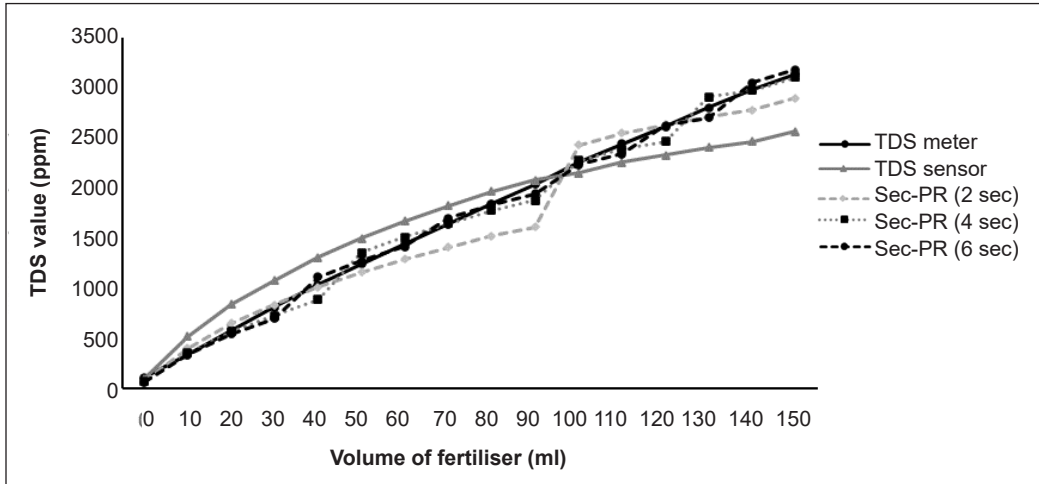


Figure 5. TDS values of Sec-PR for different numbers of sections

Sec-PR was implemented in the experimental setup to determine its performance in the real environment. The findings of the experiment are shown in Figure 6. The graph shows that the performance of Sec-PR in the experiment is comparable with the mathematical analysis. Table 3 shows that Sec-PR has recorded MAE and RMSE equal to 79.94 and 93.96, respectively, about a 67.8% improvement compared to the uncalibrated TDS value.

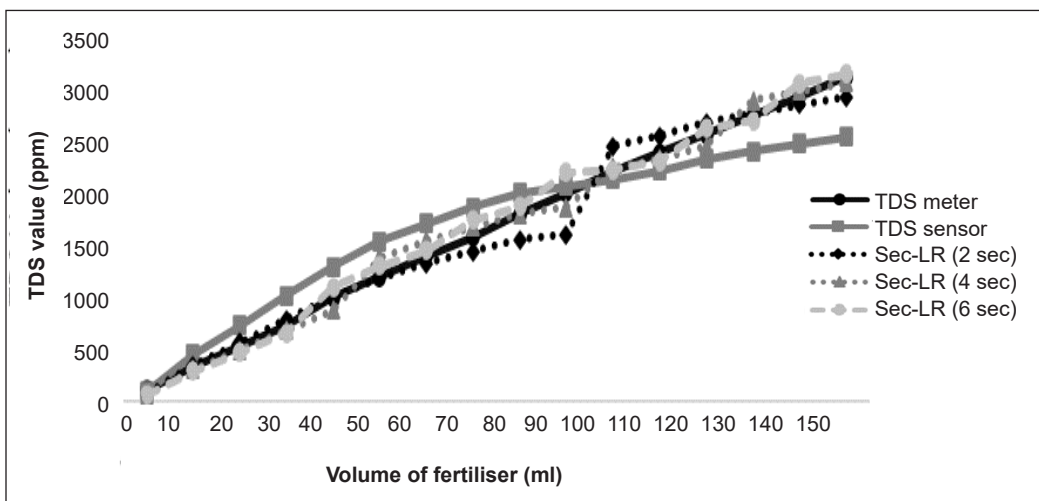


Figure 6. Experimental results of Sec-PR for different numbers of sections

The performance of Sec-PR is compared with other TDS sensor calibration methods (Table 4). Based on the literature, three calibration methods are considered for comparison: machine learning, Gaussian Process, and Multi-layer perception. The recorded MAE and RMSE values are taken directly from the literature. Sec-PR provides

comparable performances when compared to machine learning and multilayer perception. The RMSE value recorded by Sec-PR is just slightly higher when compared to machine learning and multilayer perception, which can be considered a variation in the different experimental setups. In terms of MAE, Sec-PR also gives comparable performance when compared to multilayer perception. Sec-PR and multilayer perception have recorded MAE equal to 79.94 and 40.6973, respectively. However, Sec-PR has recorded a better calibration accuracy when compared to Gaussian Process for both MAE and RMSE. Even though Sec-PR does not provide the best accuracy, Sec-PR covers a wider calibration range compared to other calibration methods.

Table 3
Experimental results of MAE and RMSE for Sec-PR

| Algorithm | MAE | RMSE |
|---------------------|--------|--------|
| TDS Sensor | 254.16 | 292.82 |
| Sec-PR (2 Sections) | 117.09 | 161.02 |
| Sec-PR (4 Sections) | 82.34 | 97.80 |
| Sec-PR (6 Sections) | 79.94 | 93.69 |

Table 4
Comparison of Performance between Sec-PR and the existing calibration methods

| Algorithm | MAE | RMSE | Range |
|---|---------|----------|---------------|
| Sec-PR | 79.94 | 93.69 | 0 to 3000 ppm |
| Machine Learning(Goparaju et al., 2021) | - | 27.93 | 0 to 400 ppm |
| Gaussian Process (Nguyen et al., 2018) | 302.681 | 352.2483 | 0 to 2000 ppm |
| Multilayer perception (Nguyen et al., 2018) | 40.6973 | 46.034 | 0 to 2000 ppm |

CONCLUSION

Sec-PR is a calibration method of TDS sensor designed for smart hydroponic systems. Sec-PR aims to extend the limited measurement range of the TDS sensor and still provide a good accuracy of sensor readings. In addition, Sec-PR can be implemented easily into any programming code of smart hydroponic systems. Sec-PR computes a polynomial regression line for TDS sensor reading over different fertilizer concentrations collected from the initial experiment. In order to map the TDS sensor reading to the TDS meter reading, the graphs are divided into several sections. Then, the average ratio between the polynomial regressed TDS sensor value, and the TDS meter value is calculated for each section. This average ratio value is implemented in the program code that will be used to calculate the calibrated value of the TDS sensor. The actual TDS sensor reading is divided by the average ratio to ensure that the sensor reading becomes almost the same as the

TDS meter. The performance of Sec-PR was determined using mathematical analysis and verified using experiments. Sec-PR provides a good accuracy of about 91% compared to the uncalibrated TDS sensor reading of just 78% accuracy. Sec-PR has recorded MAE and RMSE equal to 59.36 and 93.69, respectively. Sec-PR provides a comparable performance with Machine Learning and Multilayer Perception method. However, Sec-PR provides better performance when compared to the Gaussian Process. For future work, Sec-PR can be implemented for other types of sensors.

ACKNOWLEDGEMENTS

The project is financially supported by Universiti Tun Hussein Onn Malaysia (UTHM) under H908-TIER 1 Grant.

REFERENCES

- Alipio, M. I., Cruz, A. E. M. dela, Doria, J. D. A., & Fruto, R. M. S. (2019). On the design of Nutrient Film Technique hydroponics farm for smart agriculture. *Engineering in Agriculture, Environment and Food*, 12(3), 315-324. <https://doi.org/10.1016/j.eaef.2019.02.008>
- Daud, M., Handika, V., & Bintoro, A. (2018). Design and realization of fuzzy logic control for Ebb and flow hydroponic system. *International Journal of Scientific and Technology Research*, 7(9), 138-144.
- Domingues, D. S., Takahashi, H. W., Camara, C. A. P., & Nixdorf, S. L. (2012). Automated system developed to control pH and concentration of nutrient solution evaluated in hydroponic lettuce production. *Computers and Electronics in Agriculture*, 84, 53-61. <https://doi.org/10.1016/j.compag.2012.02.006>
- Dubey, N., & Nain, V. (2020). Hydroponic - The future of farming. *International Journal of Environment, Agriculture and Biotechnology*, 4(4), 857-864. <https://doi.org/10.22161/ijeab.54.2>
- Franchini, S., Charogiannis, A., Markides, C. N., Blunt, M. J., & Krevor, S. (2019). Calibration of astigmatic particle tracking velocimetry based on generalized Gaussian feature extraction. *Advances in Water Resources*, 124, 1-8. <https://doi.org/10.1016/j.advwatres.2018.11.016>
- Garg, K., Verma, S., & Solanki, H. A. (2021). A review on variety and variability of soil-less media for maximizing yield of greenhouse horticultural crops. *Research and Reviews: Journal of Environmental Sciences*, 3(1), 1-9. <http://doi.org/10.5281/zenodo.4663964>
- Goparaju, S. U. N., Vaddhiparthi, S. S. S., Pradeep, C., Vattem, A., & Gangadharan, D. (2021, Jun 14-July 31). *Design of an IoT system for machine learning calibrated TDS measurement in smart campus*. [Paper presentation]. 2021 IEEE 7th World Forum on Internet of Things (WF-IoT), Los Angeles, USA. <https://doi.org/10.1109/WF-IoT51360.2021.9595057>
- Graves, C. J. (1983). The nutrient film technique. *Horticultural Reviews*, 5(1), 1-44.
- Hope, T. M. (2020). *Machine learning*. Elsevier.
- Hosseini, H., Mozafari, V., Roosta, H. R., Shirani, H., van de Vlasakker, P. C. H., & Farhangi, M. (2021). Nutrient use in vertical farming: Optimal electrical conductivity of nutrient solution for growth of

- lettuce and basil in hydroponic cultivation. *Horticulturae*, 7(9), Article 283. <https://doi.org/10.3390/horticulturae7090283>
- Iida, S., Shimizu, T., Shinohara, Y., Takeuchi, S., & Kumagai, T. (2020). The necessity of sensor calibration for the precise measurement of water fluxes in forest ecosystems. *Forest-Water Interactions*, 240, 29-54. https://doi.org/10.1007/978-3-030-26086-6_2
- Karunasingha, D. S. K. (2022). Root mean square error or mean absolute error. *Information Sciences*, 585, 609-629. <https://doi.org/10.1016/j.ins.2021.11.036>
- Koestoer, R., Pancasaputra, N., Roihan, I., & Harinaldi. (2019). A simple calibration methods of relative humidity sensor DHT22 for tropical climates based on Arduino data acquisition system. *AIP Conference Proceedings*, 2062(1), Article 020009. <https://doi.org/10.1063/1.5086556>
- Maucieri, C., Nicoletto, C., van Os, E., Anseeuw, D., van Havermaet, R., & Junge, R. (2019). Hydroponic technologies. In S. Goddek, A. Joyce, B. Kotzen & G. M. Burnell (Eds.), *Aquaponics Food Production Systems* (pp.77-110). Springer. https://doi.org/10.1007/978-3-030-15943-6_4
- Modu, F., Adam, A., Aliyu, F., Mabu, A., & Musa, M. (2020). A survey of smart hydroponic systems. *Advances in Science, Technology and Engineering Systems Journal*, 5(1), 233-248. <https://doi.org/10.25046/aj050130>
- Munandar, A., Fakhurroja, H., Anto, I. F. A., Pratama, R. P., Wibowo, J. W., Salim, T. I., & Rizqyawan, M. I. (2018, November 21-22). *Design and development of an IoT-based smart hydroponic system*. [Paper presentation]. 2018 International Seminar on Research of Information Technology and Intelligent Systems (ISRITI), Yogyakarta, Indonesia. <https://doi.org/10.1109/ISRITI.2018.8864340>
- Nguyen, T. D., Nguyen, T. T. S., & Le, N. T. (2018, October 18-20). *Calibration of conductivity sensor using combined algorithm selection and hyperparameter optimization*. [Paper presentation]. 2018 International Conference on Advanced Technologies for Communications (ATC), Ho Chi Minh City, Vietnam. <https://doi.org/10.1109/ATC.2018.8587559>
- Olubanjo, O. O., Adaramola, O. D., Alade, A. E., Azubuike, C. J., & others. (2022). Development of drip flow technique hydroponic in growing cucumber. *Sustainable Agriculture Research*, 11(2), 1-67. <https://doi.org/https://doi.org/10.5539/sar.v11n2p67>
- Peršić, J., Petrović, L., Marković, I., & Petrović, I. (2021). Spatiotemporal multisensor calibration via gaussian processes moving target tracking. *IEEE Transactions on Robotics*, 37(5), 1401-1415. <https://doi.org/10.1109/TRO.2021.3061364>
- Pramono, S., Nuruddin, A., & Ibrahim, M. H. (2020). Design of a hydroponic monitoring system with deep flow technique (DFT). *AIP Conference Proceedings*, 2217(1), Article 030195. <https://doi.org/10.1063/5.0000733>
- Singh, H., & Dunn, B. (2016). *Electrical conductivity and pH guide for hydroponics* (HLA-6722). Division of Agriculture Science and Natural Resources Oklahoma State University. https://shareok.org/bitstream/handle/11244/331022/oksa_HLA-6722_2016-10.pdf
- Son, J. E., Kim, H. J., & Ahn, T. I. (2020). Hydroponic systems. In T. Kozai, G. Niu & M. Takagaki (Eds.), *Plant Factory* (pp.273-283). Academic Press. <https://doi.org/10.1016/B978-0-12-816691-8.00020-0>

- Suseno, J., Munandar, M., & Priyono, A. (2020). The control system for the nutrition concentration of hydroponic using web server. *Journal of Physics: Conference Series*, 1524(1), Article 012068. <https://doi.org/10.1088/1742-6596/1524/1/012068>
- Urban, S., Ludersdorfer, M., & van der Smagt, P. (2015). Sensor calibration and hysteresis compensation with heteroscedastic gaussian processes. *IEEE Sensors Journal*, 15(11), 6498-6506. <https://doi.org/10.1109/JSEN.2015.2455814>
- Wibowo, R. R. D. I., Ramdhani, M., Priramadhi, R. A., & Aprillia, B. S. (2019). IoT based automatic monitoring system for water nutrition on aquaponics system. *Journal of Physics: Conference Series*, 1367(1), Article 012071. <https://doi.org/10.1088/1742-6596/1367/1/012071>
- Zheng, Q., Weng, Q., & Wang, K. (2019). Developing a new cross-sensor calibration model for DMSP-OLS and Suomi-NPP VIIRS night-light imageries. *ISPRS Journal of Photogrammetry and Remote Sensing*, 153, 36-47. <https://doi.org/10.1016/j.isprsjprs.2019.04.019>